

# The Human Visual System and Adversarial AI

**Yaoshiang Ho**

*Thinky.AI Research*  
*Los Angeles, CA USA*

YAOSHIANG@THINKY.AI

**Samuel G. Wookey**

*Thinky.AI Research*  
*Los Angeles, CA USA*

SAM@THINKY.AI

**Editor:**

## Abstract

This paper applies theories about the Human Visual System to make Adversarial AI more effective. To date, Adversarial AI has modeled perceptual distances between clean and adversarial examples of images using  $L_p$  norms. These norms have the benefit of simple mathematical description and reasonable effectiveness in approximating perceptual distance. However, in prior decades, other areas of image processing have moved beyond simpler models like Mean Squared Error (MSE) towards more complex models that better approximate the Human Visual System (HVS). We demonstrate a proof of concept of incorporating HVS models into Adversarial AI.

**Keywords:** Adversarial AI, Human Visual System, Discrete Cosine Transformation, Luma, Chroma

## 1. Introduction

Adversarial AI is a set of techniques to find a small change to an input that nevertheless changes its classification by a classifier. The initial research that launched the field focused on images as the input and deep convolutional neural networks (DCNN) as the classifier (Szegedy et al., 2013).

A key to Adversarial AI is the minimization of the perceptual distance of the changes. Obviously, an unbounded change would trivially completely replace an image of say a truck with a horse. The central challenge of Adversarial AI is to change the pixels of an image of say a truck while minimizing perceptual distance, so that a human would still easily classify it as an image of a truck but a DCNN would be confused into classifying it as a horse.

The minimization of this change is often measured by  $L_p$  norms. An  $L_0$  norm counts the number of pixels changed. An  $L_1$  norm sums up the magnitude of the change over all pixels. An  $L_2$  norm is the square root of the sum of the squares of the changes. And the  $L_\infty$  norm is the magnitude of the most changed pixel. Carlini and Wagner (2017) created multiple figures that demonstrate the differences between adversarial images generated using each of these norms.

In this paper, we explore alternative perceptual distance metrics based on understandings of the human visual system (HVS). The HVS encompasses the biochemical, neurological, and psychological models of human vision. HVS is often applied to find more effective



(a) Perturbations applied to the low frequency area of the sky.

(b) Perturbations applied to the high frequency area of the rocks.

Figure 1: Example of masking in high frequencies. Identical amounts of noise have been added to both images. The perturbations in the low frequency area of the sky (left) is more noticeable than the perturbations in the high frequency area of the rocks (right) (Nadenau et al., 2000, Fig. 2).

methods of image and video compression. In image compression, there has already been a shift from simpler models like Mean Squared Error (MSE) towards more complex models that better approximate the HVS (Wang et al., 2002).

We draw on two basic theories about the HVS and find that they lead to more effective generation of adversarial data in some cases.

The first concept is that the HVS is more sensitive to lower frequency information (Figure 1). This is the basis for the discrete cosine transform (DCT) methodology of lossy image compression (Hudson et al., 2017).

The second concept is that the HVS is more sensitive to changes in luma (brightness) than chroma (hue) (Figure 2). This was discovered by Bedford (1950) during pioneering work on color television, and downsampled chroma channels continue to exist in standards today like MPEG and Apple ProRes 422 (Apple, 2018).

Our contribution is as follows. We define our problem as reducing the perceptual distance of adversarial attacks on images. Our approach is to apply HVS concepts better target the location and perturbation of adversarial attacks. In practice, this could help an adversary better hide their adversarial attacks from manual detection.

We combine two approaches into what we call the HVS2 attack. Our first approach is to only perturb pixels in high frequency zones. We use a simple model of high frequency. Our second approach is to perturb pixels to retain an approximately constant chroma. We find that these pixels are in the same "color palette" as the rest of the image, making them less detectable.



(a) A clean color image of an apple. (b) Black and white images retain the luma but eliminate chroma information. (c) An image with heavy distortion of chroma. (d) An image with chroma unchanged but luma brought to a constant level.

Figure 2: Example of luma and chroma importance. Retaining luma while eliminating or distorting chroma information results in an image that is still easily identifiable as an apple. Adjusting luma to a constant level while leaving chroma unchanged results in an image that is more difficult to classify (Zeileis et al., 2019).

The HVS2 attack works well in some cases and poorly in others.

## 2. Background and Related Work

Since its creation, the field of Adversarial AI has acknowledged the role of the HVS. In the original work of Szegedy et al. (2013) that launched the field of Adversarial AI, the authors describe adversarial images as "visually hard to distinguish".

More recently, Carlini and Wagner (2017) called for work into additional models for perceptual distance: " $L_p$  norms are reasonable approximations of human perceptual distance [...] No distance metric is a perfect measure of human perceptual similarity, and we pass no judgement on exactly which distance metric is optimal. We believe constructing and evaluating a good distance metric is an important research question we leave to future work."

In the first adversarial attack, several design choices were made. The DCNN to be attacked was analyzed by an adversary in a "whitebox" setting, meaning that the attack had access to internal values of the model not normally accessible to end users. The distance metric used was  $L_2$  norm. The input data type were images, and the specific optimization to discover the adversarial example was L-BFGS. The perturbations affected specific pixels.

Subsequent attacks have expanded the design space.

Additional optimization methods were applied, including fast gradient sign method (FGSM) (Goodfellow et al., 2014b), basic iterative method (BIM) (Kurakin et al., 2016), and projected gradient descent (PGD) (Madry et al., 2017).

The multiple options for norms were demonstrated by Carlini and Wagner (2017). Warde-Farley and Goodfellow (2016) argue that the  $L_\infty$  norm is a preferable choice for distance metric.

Additional secrecy models were introduced and attacked. If the internal values of the model are hidden, then a model can be attacked by an enhancement of finite differences called simultaneous perturbation stochastic approximation (SPSA) (Uesato et al., 2018) and boundary attack (Brendel et al., 2017). Hiding even the output of the softmax behind a top-1 hard-labeling function can be attacked (Cheng et al., 2018). Other non-differentiable layers can be approximated by backward pass differentiable approximation (BPDA) (Athalye et al., 2018).

Input types were expanded to include audio, text, and structured data (Cheng et al., 2018).

The classifier designs expanded beyond DCNN to include RNN, SVM, and gradient boosted decision trees (Papernot et al., 2016b).

A series of defenses have been proposed, including defensive distillation (Papernot and McDaniel, 2016). Nearly all have been defeated except the original approach proposed: adversarial retraining (Uesato et al., 2018) and an optimization, logit pairing (Kannan et al., 2018).

Finally, the attacks have moved beyond pixel-perfect attacks into the physical world (Kurakin et al., 2016; Eykholt et al., 2017; Tencent, 2019).

The term adversarial is also used in the field of generative adversarial nets (GANs) (Goodfellow et al., 2014a). The term adversarial is used identically in both GANs and Adversarial AI. In both fields, a generator attempts to create adversarial examples that fool a discriminator. In a GAN, the generator and discriminator are two separate deep neural networks (DNN). By comparison, in Adversarial AI the discriminator is an existing classifier and the generator is a hijacked version of the classifier itself, rather than a separate DNN. If an analogy for GANs is a counterfeiter and a cop competing with each other, the analogy for Adversarial AI is that the cop is brainwashed into using its police skills to create counterfeits.

### 3. The HVS2 Attack

We chose the generic DCNN architecture specified in the Keras documentation for its small computational complexity. We ran our attack on 100 images from CIFAR10 (Krizhevsky et al.). We used ourselves as the human subjects to qualitatively measure perceptual distance.

We based our attacks on the FGSM method for its low computational requirements. For ease of implementation, we implemented FGSM ourselves rather than modify the reference implementation in cleverhans (Papernot et al., 2016a).

Our HSV2 attack combines hiding perturbations in high frequency areas and constant chroma.

For hiding perturbations in high frequency areas, we built our own simple measure of high frequency. For each pixel’s color channel, we calculated two means: the mean of the above and below pixel’s color channels, and the mean of the left and right color channels. We ignored pixels on the edges and corners.

With the vertical mean and horizontal mean in hand, we calculated the absolute value of the pixel channel’s deviation from each of these means. Then we took the min of those two deviations. This is our approximation of frequency for each color channel per pixel.

Layer Type	Hyperparameters
Convolution + Relu	32x3x3
Convolution + Relu	32x3x3
Maxpool	2x2
Dropout	0.25
Convolution + Relu	64x3x3
Convolution + Relu	64x3x3
Maxpool	2x2
Dropout	0.25
Flatten	
Dense	512
Dropout	0.5
Dense + Softmax	10

Table 1: Our DCNN architecture.

For each pixel, we took the max of the frequencies of the three color channels. This is our approximation of frequency for a pixel. We reasoned that even if the channel frequencies from say red and green were low, a high frequency for the blue channel would still cause the HVS to perceive high frequency for the pixel.

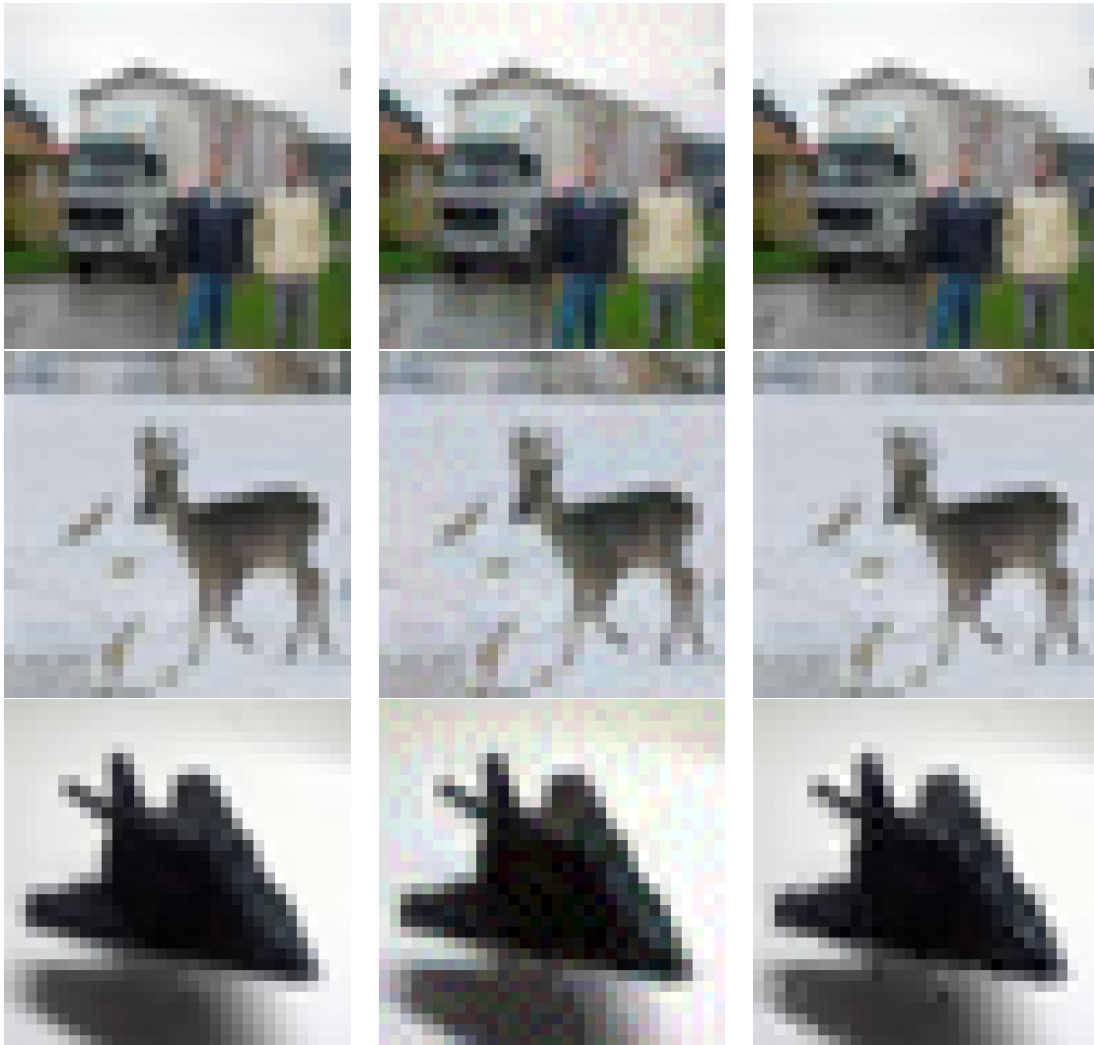
With an estimate of frequency for each individual pixel, we only allowed FGSM to adjust pixels that had a higher than a specific threshold. Any pixel with a lower frequency was not perturbed. We tried several thresholds and found 0.01 to generate reasonable results for some images.

As described below, our initial hypothesis of constant luma failed to product effective results but led us to the approach of constant chroma. We approximated constant chroma by only allowing FGSM to operate on pixels where the sign of the gradients on all three color channels were either positive or negative. We reason that constant chroma creates perturbed pixels within the same color palette as the rest of the image, reducing perceptual distance.

We found that the majority of the FGSM adversarial examples were indistinguishable. For the handful of FGSM examples that were distinguishable, the HVS2 attack would sometimes successfully generate better images (less perceptual distance) images. Other times, it would generate worse images (more perceptual distance). See Figures 3 and 4 for examples of each.

#### 4. Other approaches that failed

Our initial hypothesis on luma and chroma was to convert the image pixels from RGB to YUV, an HSV oriented colormap that separate luma (Y) from chroma (U and V). To implement that hypothesis, we converted the gradients generated by FGSM into YUV space, then clipped to zero any perturbations to the Y (luma) channel. We used the Tensorflow implementation (Abadi et al., 2015), which uses the matrices in Equations 1 and 2. To apply

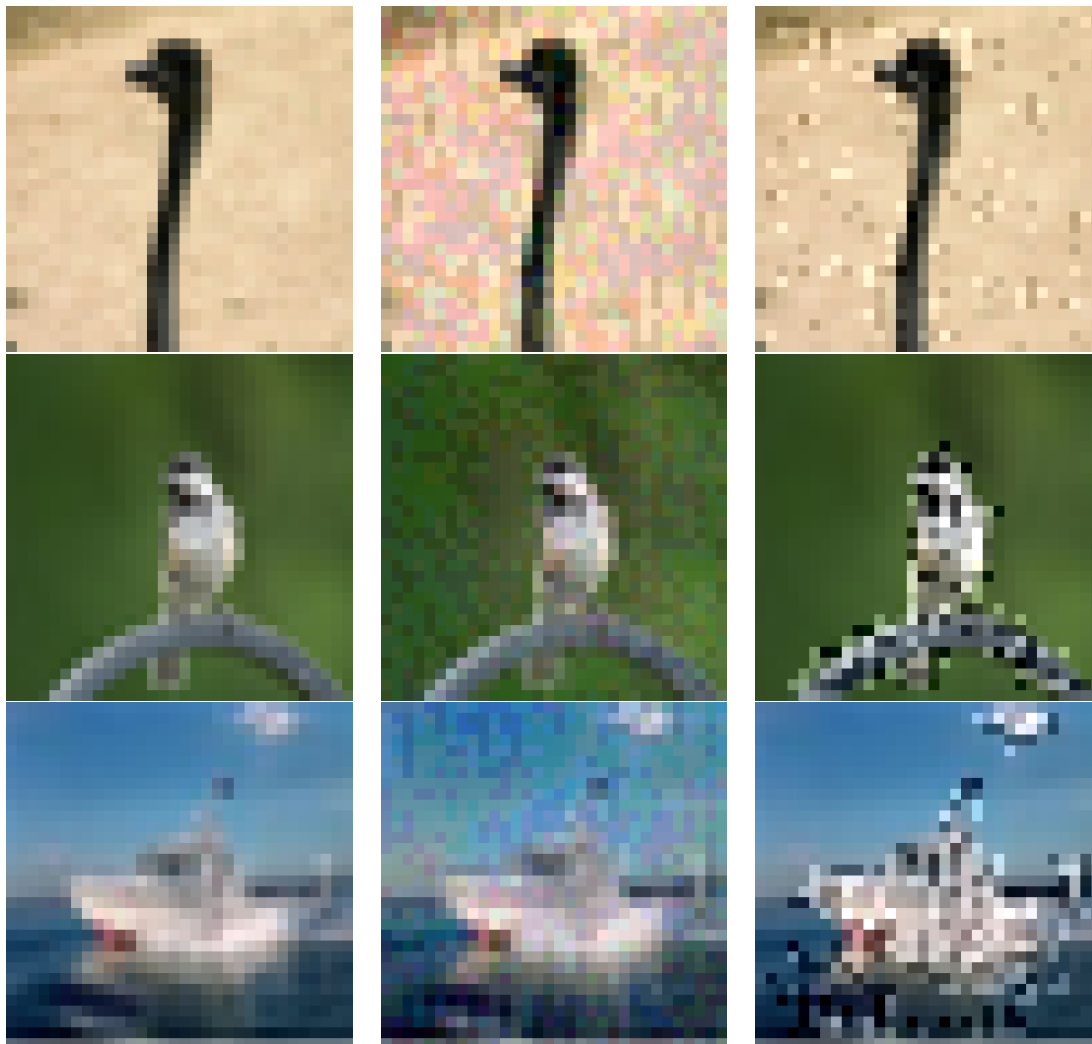


(a) Original images.

(b) FGSM attack.

(c) HVS2 attack.

Figure 3: The good results. The clean images in column (a) show "smooth" low frequency regions. The FGSM attacked images in column (b) show "rainbow snow" in those regions. The HVS2 attacked images in column (c) reduce chroma changes and hide adversarial pixels in high frequency areas, leading to lower perceptual distance. Original image size 32x32.



(a) Original images.

(b) FGSM attack.

(c) HVS2 attack.

Figure 4: The bad results. The clean images in column (a) don't have enough high frequency areas to hide adversarial pixels. The HVS2 attacked images in column (c) attempt to place adversarial pixels in the few low frequency pixels, leading to large perturbations. Original image size 32x32.

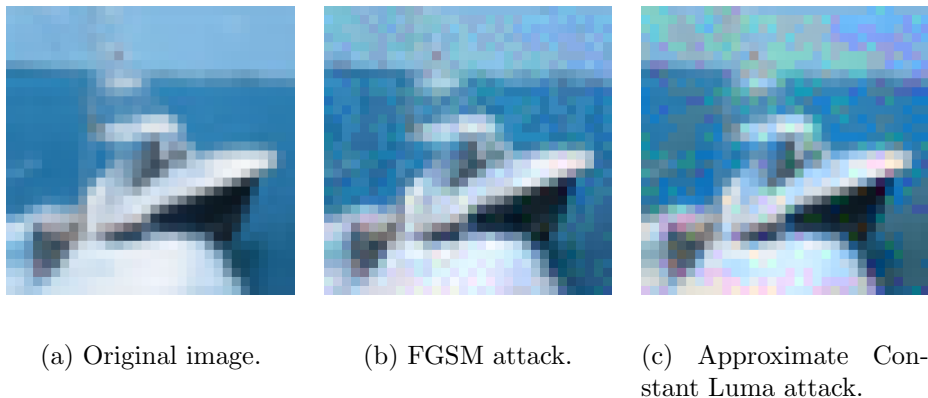


Figure 5: Example of results from an approximate constant luma attack. The "rainbow snow" texture of Approximate Constant Luma attacked image (c) is worse than the FGSM attacked image (b). Original image size 32x32.

the YUV perturbations, we would take our RGB image, generate a YUV image, apply the YUV perturbations, then convert back to RGB.

$$\begin{bmatrix} Y \\ U \\ V \end{bmatrix} = \begin{bmatrix} 0.299 & 0.587 & 0.114 \\ -0.14714119 & -0.28886916 & 0.43601035 \\ 0.61497538 & -0.51496512 & -0.10001026 \end{bmatrix} \begin{bmatrix} R \\ G \\ B \end{bmatrix} \quad (1)$$

$$\begin{bmatrix} R \\ G \\ B \end{bmatrix} = \begin{bmatrix} 1 & 0 & 1.13988303 \\ 1 & -0.394642334 & -0.58062185 \\ 1 & 2.03206185 & 0 \end{bmatrix} \begin{bmatrix} Y \\ U \\ V \end{bmatrix} \quad (2)$$

Using this approach, FGSM was generally not able to find an adversarial example. We hypothesize that the conversion between RGB and YUV acts as a hash function, reducing the overall effect of any perturbation on a DCNN trained on RGB images.

Our second approach was to approximate our constant luma approach by searching for pixels where one of the three RGB channels was positive and one was negative. Obviously, this approach ignores clipping as well as the relatively higher luma of green pixels and lower luma of blue pixels. This attack created colorized textures that created more perceptual distance. See Figure 5. However, we hypothesized that perhaps the theory of luma and chroma needed to be revised in the context of Adversarial AI. While changes in chroma may indeed be less noticeable to the human eye than luma, changing luma but retaining chroma would generally create perturbations within the same color palette which would be easier to hide in high frequency areas. The result was the perturbations described in the previous section.

## 5. Conclusion and future work

In this paper, we have modified adversarial AI attacks to incorporate HVS theories of perceptual distance. We have found that simple approaches can be effective at yielding

images that are less detectable by the human visual system. By design, these approaches are simple and unoptimized. We believe better results are possible through many directions for future work.

Many existing models of the HVS can be used in lieu of  $L_p$  norms to optimize for a weighted average of both misclassification and perceptual distance using PGD (Nadenau et al., 2000). Even the common approach of DCT will likely outperform our simple measure of frequency (Hudson et al., 2017).

Continuous clipping functions can be used for for adversarial perturbations. Our current approach essentially clips away all adversarial perturbation outside of known regions. Instead, we could allow smaller perturbations in lower frequency areas and larger perturbations in higher frequency areas.

Because people are accustomed to JPEG compression artifacts, it may be possible to hide perturbations even in low frequency areas of images if boxed in by 8x8 pixel regions to simulate the artifacts of JPEG compression.

Existing HVS models were mainly focused on quality of image compression. There may be different HVS models for hiding adversarial perturbations. To promote further research, new mathematically HVS models focused on hiding adversarial perturbations can be developed. Initially these models will need to be benchmarked by human subjects, just like existing HVS models (Sheikh et al., 2006).

DCNNs trained on on HVS-based colorspace like YUV may be require larger perceptual distance to generate adversarial perturbations.

Finally, outside the field of Adversarial AI, the relatively importance of luma suggests a new design for convolutional neural networks, where the luma channel has relatively more hidden layers and more weights than the chroma channels. In an extreme model, chroma could be eliminated entirely to train a black and white only DCNN.

## Acknowledgments

We would like to acknowledge support for this project from Tom Rikert, Chiara Cerini, David Wu, Bjorn Eriksson, and Israel Nizenz.

## References

- Martín Abadi, Ashish Agarwal, Paul Barham, Eugene Brevdo, Zhifeng Chen, Craig Citro, Greg S. Corrado, Andy Davis, Jeffrey Dean, Matthieu Devin, Sanjay Ghemawat, Ian Goodfellow, Andrew Harp, Geoffrey Irving, Michael Isard, Yangqing Jia, Rafal Jozefowicz, Lukasz Kaiser, Manjunath Kudlur, Josh Levenberg, Dandelion Mané, Rajat Monga, Sherry Moore, Derek Murray, Chris Olah, Mike Schuster, Jonathon Shlens, Benoit Steiner, Ilya Sutskever, Kunal Talwar, Paul Tucker, Vincent Vanhoucke, Vijay Vasudevan, Fernanda Viégas, Oriol Vinyals, Pete Warden, Martin Wattenberg, Martin Wicke, Yuan Yu, and Xiaoqiang Zheng. TensorFlow: Large-scale machine learning on heterogeneous systems, 2015. URL <https://www.tensorflow.org/>. Software available from tensorflow.org.
- Apple. Apple prores white paper, 2018. URL [https://www.apple.com/final-cut-pro/docs/Apple\\_ProRes\\_White\\_Paper.pdf](https://www.apple.com/final-cut-pro/docs/Apple_ProRes_White_Paper.pdf).
- Anish Athalye, Nicholas Carlini, and David Wagner. Obfuscated gradients give a false sense of security: Circumventing defenses to adversarial examples. *arXiv preprint arXiv:1802.00420*, 2018.
- Alda V Bedford. Mixed highs in color television. *Proceedings of the IRE*, 38(9):1003–1009, 1950.
- Wieland Brendel, Jonas Rauber, and Matthias Bethge. Decision-based adversarial attacks: Reliable attacks against black-box machine learning models. *arXiv preprint arXiv:1712.04248*, 2017.
- Nicholas Carlini and David Wagner. Towards evaluating the robustness of neural networks. In *2017 IEEE Symposium on Security and Privacy (SP)*, pages 39–57. IEEE, 2017.
- Minhao Cheng, Thong Le, Pin-Yu Chen, Jinfeng Yi, Huan Zhang, and Cho-Jui Hsieh. Query-efficient hard-label black-box attack: An optimization-based approach. *arXiv preprint arXiv:1807.04457*, 2018.
- Kevin Eykholt, Ivan Evtimov, Earlene Fernandes, Bo Li, Amir Rahmati, Chaowei Xiao, Atul Prakash, Tadayoshi Kohno, and Dawn Song. Robust physical-world attacks on deep learning models. *arXiv preprint arXiv:1707.08945*, 2017.
- Ian Goodfellow, Jean Pouget-Abadie, Mehdi Mirza, Bing Xu, David Warde-Farley, Sherjil Ozair, Aaron Courville, and Yoshua Bengio. Generative adversarial nets. In *Advances in neural information processing systems*, pages 2672–2680, 2014a.
- Ian J Goodfellow, Jonathon Shlens, and Christian Szegedy. Explaining and harnessing adversarial examples. *arXiv preprint arXiv:1412.6572*, 2014b.
- Graham Hudson, Alain Lger, Birger Niss, and Istvan Sebestyen. Jpeg at 25: Still going strong. *IEEE MultiMedia*, 24:96–103, 04 2017. doi: 10.1109/MMUL.2017.38.
- Harini Kannan, Alexey Kurakin, and Ian Goodfellow. Adversarial logit pairing. *arXiv preprint arXiv:1803.06373*, 2018.

- Alex Krizhevsky, Vinod Nair, and Geoffrey Hinton. Cifar-10 (canadian institute for advanced research). URL <http://www.cs.toronto.edu/~kriz/cifar.html>.
- Alexey Kurakin, Ian Goodfellow, and Samy Bengio. Adversarial examples in the physical world. *arXiv preprint arXiv:1607.02533*, 2016.
- Aleksander Madry, Aleksandar Makelov, Ludwig Schmidt, Dimitris Tsipras, and Adrian Vladu. Towards deep learning models resistant to adversarial attacks. *arXiv preprint arXiv:1706.06083*, 2017.
- Marcus J Nadenau, Stefan Winkler, David Alleysson, and Murat Kunt. Human vision models for perceptually optimized image processing—a review. *Proceedings of the IEEE*, 32, 2000.
- Nicolas Papernot and Patrick McDaniel. On the effectiveness of defensive distillation. *arXiv preprint arXiv:1607.05113*, 2016.
- Nicolas Papernot, Fartash Faghri, Nicholas Carlini, Ian Goodfellow, Reuben Feinman, Alexey Kurakin, Cihang Xie, Yash Sharma, Tom Brown, Aurko Roy, et al. Technical report on the cleverhans v2. 1.0 adversarial examples library. *arXiv preprint arXiv:1610.00768*, 2016a.
- Nicolas Papernot, Patrick McDaniel, and Ian Goodfellow. Transferability in machine learning: from phenomena to black-box attacks using adversarial samples. *arXiv preprint arXiv:1605.07277*, 2016b.
- Hamid R Sheikh, Muhammad F Sabir, and Alan C Bovik. A statistical evaluation of recent full reference image quality assessment algorithms. *IEEE Transactions on image processing*, 15(11):3440–3451, 2006.
- Christian Szegedy, Wojciech Zaremba, Ilya Sutskever, Joan Bruna, Dumitru Erhan, Ian Goodfellow, and Rob Fergus. Intriguing properties of neural networks. *arXiv preprint arXiv:1312.6199*, 2013.
- Tencent. Experimental security research of tesla autopilot, 2019. URL [https://keenlab.tencent.com/en/whitepapers/Experimental\\_Security\\_Research\\_of\\_Tesla\\_Autopilot.pdf](https://keenlab.tencent.com/en/whitepapers/Experimental_Security_Research_of_Tesla_Autopilot.pdf).
- Jonathan Uesato, Brendan O’Donoghue, Aaron van den Oord, and Pushmeet Kohli. Adversarial risk and the dangers of evaluating against weak attacks. *arXiv preprint arXiv:1802.05666*, 2018.
- Zhou Wang, Alan C Bovik, and Ligang Lu. Why is image quality assessment so difficult? In *2002 IEEE International Conference on Acoustics, Speech, and Signal Processing*, volume 4, pages IV–3313. IEEE, 2002.
- David Warde-Farley and Ian Goodfellow. 11 adversarial perturbations of deep neural networks. *Perturbations, Optimization, and Statistics*, 311, 2016.

Achim Zeileis, Jason C Fisher, Kurt Hornik, Ross Ihaka, Claire D McWhite, Paul Murrell, Reto Stauffer, and Claus O Wilke. colorspace: A toolbox for manipulating and assessing colors and palettes. *arXiv preprint arXiv:1903.06490*, 2019.